Photoelectron spectroscopy of Si_nH^- ($n=2-4$) anions

Cangshan Xu,[a] Travis R. Taylor, Gordon R. Burton,[b] and Daniel M. Neumark
Department of Chemistry, University of California, Berkeley, California 94720 and Chemical Sciences Division, Lawrence Berkeley Laboratory, Berkeley, California 94720

(Received 25 November 1997; accepted 5 February 1998)

Vibrationally resolved photoelectron spectra of Si_nH^- ($n=2-4$) have been measured at a photodetachment wavelength of 355 nm (3.493 eV). The electron affinities of Si_2H, Si_3H, and Si_4H are 2.31 ± 0.01, 2.53 ± 0.01, and 2.68 ± 0.01 eV, respectively. Vibrational frequencies for the neutral ground states and a low-lying state of Si_2H are also determined. Assignment of the electronic states and vibrational frequencies is facilitated by comparison with *ab initio* calculations. The calculations show that the H atom in Si_4H and Si_4H^- is bonded to a single Si atom, in contrast to the bridged structures found for the smaller clusters. These calculations, along with photoelectron energy and angular distributions, yield a definitive assignment of the ground and nearly degenerate first excited states of Si_2H. © *1998 American Institute of Physics.* [S0021-9606(98)01818-2]

I. INTRODUCTION

Silicon hydrides serve as reaction intermediates in chemical vapor deposition of amorphous silicon from silanes.[1] Silicon hydride anions have been implicated in the formation of dust particles in the plasma etching and deposition of silicon.[2,3] A full understanding of the reaction mechanisms in these processes requires the characterization of the ground and low-lying electronic states of the neutral and negatively charged silicon hydrides. In addition, the nature of the silicon–hydrogen bonding in silicon hydrides containing more than one Si atom is of significant interest. High resolution spectra have been obtained for disilyne (Si_2H_2),[4] and numerous theoretical studies of this molecule have been carried out;[5,6] these indicate a ''dibridged'' structure in which each H atom is bound to two Si atoms.

In this paper we present experimental studies of silicon monohydrides (Si_nH) using negative ion photoelectron spectroscopy. Although there have been a small number of theoretical studies of these species,[7–9] they have proved resistant to experimental characterization due to their high reactivity. *Ab initio* calculations predict Si_2H and Si_3H to have hydrogen-bridged ground states for both neutral and anion.[7–9] This differs from the single Si–H bonds favored in the bonding of hydrogen to extended silicon surfaces.[10–15] The calculations also predict that the silicon core structures differ only slightly from the bare silicon clusters in these small silicon monohydride systems. However, the two studies[8,9] of Si_2H do not agree on the neutral ground state assignment.

The work presented here represents the first spectroscopic investigation of silicon monohydrides. We report anion photoelectron spectra of Si_2H^-, Si_3H^-, and Si_4H^- at a photodetachment wavelength of 355 nm (3.493 eV). We have obtained electron affinities and vibrational frequencies of the ground states for all three silicon monohydrides. Photoelectron angular distributions were used to distinguish transitions to the nearly degenerate ground and first excited states of Si_2H. *Ab initio* calculations were also performed on the three anion and neutral species to aid in assigning the electronic and vibrational structure in the photoelectron spectra.

II. EXPERIMENT

The experiments were carried out on a time-of-flight negative ion photoelectron spectrometer.[16,17] The anions of interest are generated by expanding a dilute mixture of SiH_4 (5% SiH_4, 95% He) through a pulsed piezoelectric valve/pulsed electrical discharge source.[18] In this source, the gas pulse from the beam valve passes through two stainless steel plates between which a high voltage (about 600 V) pulse is applied. The pulse then expands into a vacuum chamber. The resulting free jet is collimated by a 2 mm diameter skimmer located 1.5 cm downstream from the ion source and then enters a differentially pumped region. Here, the ions are extracted from the beam and enter a time-of-flight mass spectrometer with a linear reflectron stage; the overall mass resolution is $\sim$2000. The accelerated ions separate in time and space according to their mass to charge ratios, and are selectively detached by a pulsed Nd:YAG laser.

The third harmonic (355 nm, 3.493 eV) from a pulsed Nd:YAG laser is used in these experiments. The photoelectron kinetic energy is measured by time-of-flight in a field-free flight tube 100 cm in length. The instrumental resolution is 8–10 meV for an electron kinetic energy (eKE) of 0.65 eV and degrades as $(\mathrm{eKE})^{3/2}$. The polarization angle θ between the laser polarization and the direction of electron collection can be varied using a half-wave plate. The variation of peak intensities with θ is used to separate the contributions of different electronic states to the photoelectron spectra.

III. RESULTS

The anion mass spectrum obtained from the discharge source is shown in Fig. 1. Bare silicon clusters as well as

[a]Current address: Lam Research Corporation, 47131 Bayside Parkway, Fremont, CA 94538.
[b]Current address: Whiteshell Laboratories, Pinawa, Manitoba, ROE 1L0, Canada.

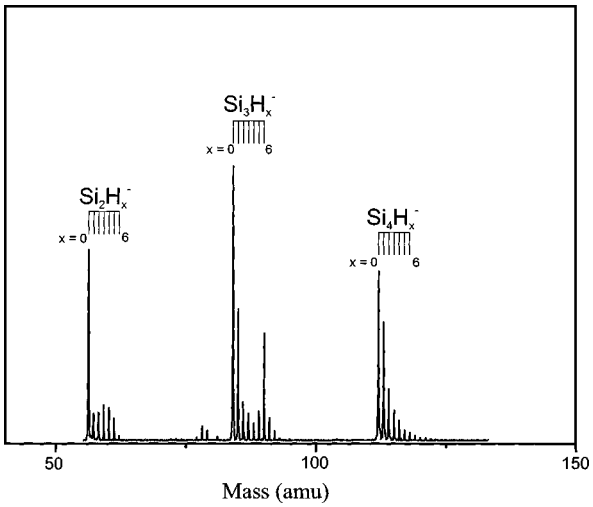

FIG. 1. Mass spectra of silicon hydride anions and corresponding bare silicon anion clusters generated from the discharge ion source.

partially hydrogenated species $Si_xH_y^-$ are observed. Since silicon has three isotopes with atomic mass units (amu) of 28 (92%), 29 (5%), and 30 (3%), respectively, the silicon hydride mass peaks in the mass spectrum are contaminated by bare silicon clusters with the same number of Si atoms. The peak at 57 amu, for example, is a mixture of $^{28}Si_2H^-$ and $^{28}Si^{29}Si^-$ anions. The photoelectron spectrum for Si_2H^- can be obtained by subtracting the appropriately scaled Si_2^- spectrum at 56 amu from the spectrum at 57 amu, and likewise for the larger clusters. Figure 2 shows the raw spectra (top panel), the Si_n^- spectra (middle panel), and the Si_nH^- ($n=2-4$) spectra after subtraction (bottom panel). The spectra shown in Fig. 2 were taken at laser polarization angle $\theta=54.7°$ (magic angle).

The Si_nH^- spectra consist of bands corresponding to transitions from the anion to various neutral electronic states. Vibrational structure is resolved in many of these bands. For each peak, the electron kinetic energy (eKE) is given by:

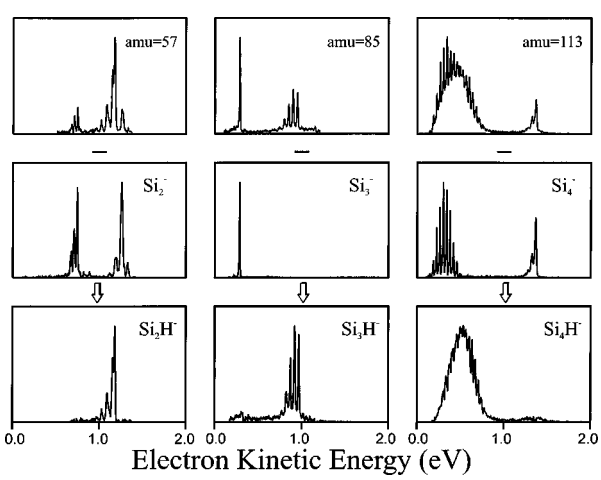

FIG. 2. Photoelectron spectra of Si_nH^- ($n=2-4$) taken at 355 nm. Laser polarization angle θ is 55° (magic angle) with respect to direction of electron collection. The three rows show how the Si_nH^- spectra are generated by subtracting the corresponding Si_n^- spectrum (see text for details).

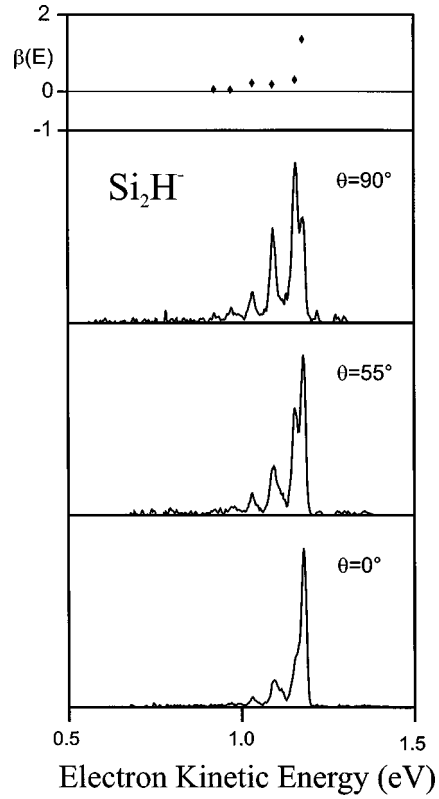

FIG. 3. Photoelectron spectra of Si_2H^- taken at 355 nm. Laser polarization angles are $\theta=90$, 55, and 0°. Top panel shows anisotropy parameters β for each peak in the spectrum.

$$\mathrm{eKE}=h\nu-\mathrm{EA}-E_v^{(0)}+E_v^{(-)}-T_0^{(0)}+T_0^{(-)}, \tag{1}$$

where $h\nu$ is the laser photon energy (3.493 eV), EA is the adiabatic electron affinity of the neutral species, and $E_v^{(0)}$ and $E_v^{(-)}$ are the neutral and anion vibrational energies, respectively, above the zero point energy. For photodetachment transitions between electronically excited neutral and/or anion states, $T_0^{(0)}$ and $T_0^{(-)}$ are the excited state term values defined with respect to the neutral and anion electronic ground states, respectively.

The photoelectron angular distribution is given by[19]

$$\frac{d\sigma}{d\Omega}=\frac{\sigma_{\mathrm{total}}}{4\pi}[1+\beta(E)P_2(\cos\theta)], \tag{2}$$

where σ_{total} is the total photodetachment cross section, θ is measured with respect to the laser polarization, and $\beta(E)$ is the asymmetry parameter, varying from -1 to 2. One can determine β for each peak in the photoelectron spectrum through its intensity variation with laser polarization angle.

Of the three anions studied here, Si_2H^- shows the most interesting photoelectron angular distribution, as shown in the spectra in Fig. 3 taken at three laser polarization angles. These spectra consist of two overlapping bands with different photoelectron angular distributions. The top panel shows that the β parameters for the two bands, hereafter referred to as bands X and A, are 1.4 and ~ 0, respectively. Band X is dominated by its vibrational origin at $\mathrm{eKE}=1.18\pm0.01$ eV.

TABLE I. QCISD(T)/6-31G* optimized geometries, frequencies, and normal coordinate displacements for Si_2H. Anion and neutral energies are derived from the QCISD(T)/6-311+G(3*DF*) energies using the QCISD(T)/6-31G* optimized geometries, and are defined relative to the neutral ground electronic state.

	States	E (eV)	R_{Si-H} (Å)	R_{Si-Si} (Å)	∠SiHSi	Frequencies (cm^{-1})/ΔQ (Å·$amu^{1/2}$) ν_1	ΔQ_1	ν_2	ΔQ_2	ν_3
Si_2H^-	$^1A_1(C_{2v})$	−2.25	1.690	2.182	80.4°	1479		558		1103
Ref. 8			1.706	2.215	81.0°					
Si_2H	$^2A_1(C_{2v})$	0.0	1.693	2.155	79.1°	1592	0.01	554	0.10	1048
Ref. 8			1.708	2.194	79.4°					
Ref. 9			1.658	2.123	79.6°					
	$^2B_1(C_{2v})$	0.01	1.703	2.241	82.3°	1491	0.01	525	0.22	1032
Ref. 8			1.723	2.273	82.6°					
Ref. 9			1.677	2.218	82.4°					

Band A, which is most apparent at $\theta=90°$, consists of a more extended progression of five peaks, starting at 1.16 ±0.01 eV and spaced by 520±20 cm^{-1}.

The Si_3H^- spectrum in Fig. 2 shows a single band with its origin at 0.97±0.01 eV electron energy. A vibrational progression of five peaks spaced by 398±20 cm^{-1} is clearly resolved. Measurement of the photoelectron angular distributions shows that all peaks have approximately the same anisotropy, with an average β parameter of −0.4. The base line noise at low eKE (~0.3 eV) results from background subtraction of a strong Si_3^- transition.

The Si_4H^- spectrum in Fig. 2 shows a single band. Eight peaks with a spacing of 310±20 cm^{-1} are apparent starting at eKE=0.81±0.01 eV; the structure below 0.5 eV is more irregular. The average anisotropy parameter for this band is $\beta=-0.4$.

In order to aid assignments of electronic and vibrational structure, we performed geometry optimization and frequency calculations on each anion and neutral at the QCISD(T)/6-31G* level of theory, using the GAUSSIAN 94 package.[20] The optimized geometries are then adopted to obtain more reliable electronic state energies using a larger basis set of 6-311+G(3*DF*) at the same level of theory. For Si_4H and Si_4H^-, a ground state structure search was performed at the MP2/6-31G* level. The results are summarized in Tables I–III. The geometries of the silicon monohydride clusters used in these tables are shown in Figs. 4–6. These calculations also yield normal coordinate displacements for photodetachment to each neutral state. The displacements are calculated within the parallel mode approximation, in which the force constants for the neutral state are assumed for both the anion and neutral. One can then perform Franck–Condon simulations of the spectrum based on the *ab initio* calculations and compare them with experiment. All simulations assume no vibrational excitation of the anions. The electron affinities and adiabatic excitation energies from the calculations aid in the assignments of electronic states. This type of comparison with theory proved very useful in our recent work on Si_n^- photoelectron spectroscopy.[21]

IV. ANALYSIS AND DISCUSSION

A. General

In this section, the photoelectron spectra will be analyzed and assigned to various electronic states. The ground state structures of anions and neutrals are determined by *ab initio* calculations. Franck–Condon simulations provide vibrational profiles, which are very helpful in assigning the spectra. For Si_2H^-, the assignments of overlapped bands were aided by photoelectron angular distributions. The discussion is concluded by comparisons between the bare silicon clusters and the silicon monohydrides.

B. Si_2H^-

Figure 3 shows transitions to two nearly degenerate electronic states of Si_2H. Both bands are well resolved, but the

TABLE II. QCISD(T)/6-31G* optimized geometries, frequencies, and normal coordinate displacements for Si_3H/Si_3H^- and Si_3/Si_3^-.[a] Anion and neutral energies are derived from the QCISD(T)/6-311+G(3*DF*) energies using the QCISD(T)/6-31G* optimized geometries and are defined relative to the neutral ground electronic state.

	States	E (eV)	$R(1-2)$ (Å)	$R(1-3)$ (Å)	$R(1-H)$ (Å)	∠(1−H−2)	Frequencies (cm^{-1})/ΔQ(Å·$amu^{1/2}$)
Si_3H^-	$^1A_1$ (C_{2v})	−2.48	2.498	2.284	1.699	94.7°	1410(a_1),521(a_1),379(a_1),952(b_2),539(b_1),411(b_2)
Si_3H	$^2B_2$ (C_{2v})	0.0	2.403	2.305	1.667	92.2°	1499(a_1)/0.02,498(a_1)/0.02,409(a_1)/0.42,1003(b_2), 463(b_1),301(b_2)
Si_3^-	$^2A_1$ (C_{2v})	−2.21	2.437	2.261			533(a_1),297(a_1),370(b_2)
Si_3	$^3A_2'$ (D_{3h})	0.02	2.290	2.290			522(a_1),285(e)

[a]Reference 27.

TABLE III. MP2/6-31G* optimized geometries, frequencies, and normal coordinate displacements for Si_4H/Si_4H^- and Si_4/Si_4^-.[a] Anion and neutral energies are derived from the QCISD(T)/6-311+G(3*DF*) energies using the MP2/6-31G* optimized geometries and are defined relative to the neutral ground electronic state.

	States	E (eV)	$R(1-2)$ (Å)	$R(1-3)$ (Å)	$R(2-3)$ (Å)	$R(2-4)$ (Å)	$R(1-\mathrm{H})$ (Å)	$\angle(\mathrm{H}-1-3)$	Frequencies $(\mathrm{cm}^{-1})/\Delta Q(\text{Å}\cdot\mathrm{amu}^{1/2})$[b]
Si_4H^-	$^1A'$ (C_s)	−2.53	2.391	4.020	2.274	2.366	1.535	96.6°	1919(a'),603(a'),520(a'),504(a''),446(a'), 410(a''),335(a'),237(a''),143(a')
Si_4H	$^2A'$ (C_s)	0.0	2.313	3.839	2.263	2.492	1.500	125.1°	2100(a')/0.16,1291(a''),727(a''),537(a')/ 0.10,510(a')/0.64,448(a')/0.15,385(a''), 314(a')/0.79,142(a')/0.18
Si_4^-	$^2B_{2g}$ (D_{2h})	−2.06	2.303	3.960	2.303	2.352			485(a_g),361(a_g)
Si_4	$^3B_{3u}$ (D_{2h})	0.85	2.265	3.748	2.265	2.544			480(a_g),330(a_g)[c]

[a]Reference 27.
[b]MP2 frequencies are scaled by 0.95.
[c]QCISD/6-31G$*$ frequencies from private communication with C. Rohlfing.

origins are separated by only 0.02 eV. However, band A has a noticeably longer progression than band X, indicating a larger geometry change upon photodetachment to band A.

Ab initio calculations have been performed previously on Si_2H^- and the low-lying states of Si_2H.[8,9,22] The anion ground state is predicted to have the symmetrically bridged (C_{2v}) structure shown in Fig. 4. The valence electron configuration is $\ldots(5b_2)^2(6a_1)^2(7a_1)^2(2b_1)^2$, resulting in a $^1A_1$ state. The $^2B_1$ and $^2A_1$ states of the neutral, both of which are also predicted to have this bridged C_{2v} structure, are formed by photodetachment from the $2b_1$ and $7a_1$ orbitals, respectively. As shown in Fig. 4, the $2b_1$ orbital is a π-bonding orbital between the two Si atoms, while the $7a_1$ orbital is a σ-orbital. Previous *ab initio* calculations (see Table I) predict the two neutral states to be nearly isoenergetic. Kalcher and Sax found the $^2A_1$ state to be 0.02 eV more stable than the $^2B_1$ state, using complete active space self-consistent field (CASSCF) geometry optimization followed by multireference configuration interaction (MRCI) evaluation of the energies.[8] A later study by Ma *et al.* at the TZ2P (f,d) coupled-cluster single double (CCSD) level of theory predicted that the $^2B_1$ state lies 0.07 eV lower in energy.[9] Our higher level calculations, also summarized in Table I, predict the $^2A_1$ state to be the ground state, but only by 0.01 eV. With such a small splitting, one cannot definitively assign the ground state based solely on the calculated energetics. Moreover, the experimental peak spacing of 520 $\pm 20\ \mathrm{cm}^{-1}$ in band A can be assigned to the υ_2 Si–Si stretching mode of either state.

However, the *ab initio* calculations also show that photodetachment to the $^2A_1$ state results in a smaller geometry change than to the $^2B_1$ state. Our calculations in Table I show that $R_{\mathrm{Si-Si}}$ decreases by 0.027 Å upon detachment to the $^2A_1$ and increases by 0.059 Å upon detachment to the $^2B_1$ state. As a result, the calculated normal coordinate displacement ΔQ_2 is substantially larger for the $^2B_1$ state, 0.22 vs. 0.10 amu $\text{Å}^{1/2}$ for the $^2A_1$ state. Since a larger normal coordinate displacement produces a longer progression, we assign band X to the $^2A_1$ state and band A to the $^2B_1$ state, which is also consistent with our energy calculations. The resulting electron affinity of 2.31 ± 0.01 eV agrees well with the value of 2.25 eV from our calculations, and slightly above the MRCI(D) values of 2.14 eV by Kalcher and Sax.[8] The electron affinity of Si_2H is 0.11 eV higher than that for Si_2, 2.20 eV.[23]

Franck–Condon simulations of these two electronic transitions are superimposed on the experimental spectrum in

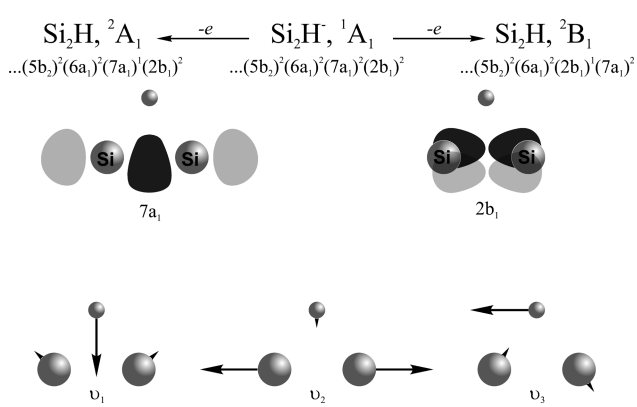

FIG. 4. High-lying electronic orbitals (top) of Si_2H/Si_2H^- and vibrational modes (bottom).

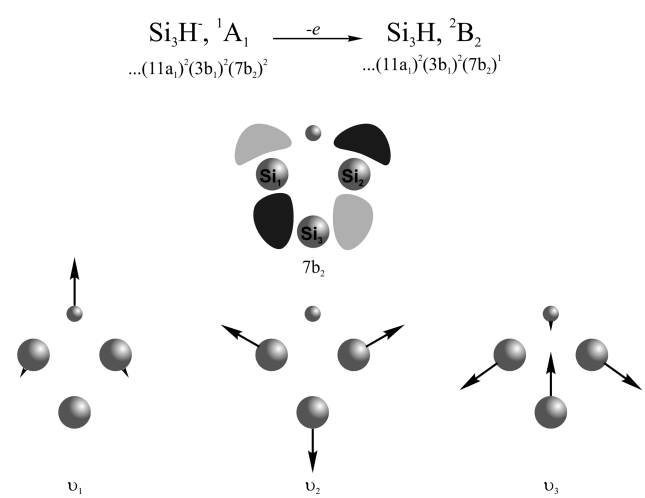

FIG. 5. HOMO of Si_3H/Si_3H^- (top) and totally symmetric vibrational modes (bottom).

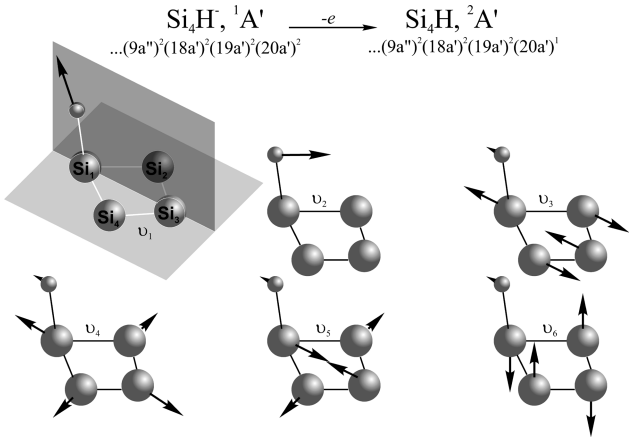

FIG. 6. HOMO of Si_4H/Si_4H^- and totally symmetric vibrational modes (bottom).

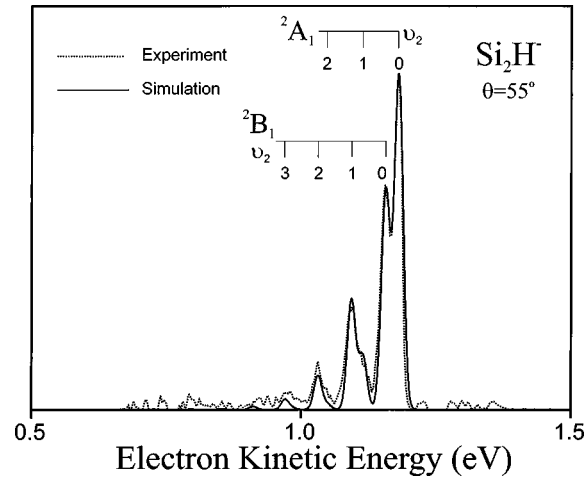

FIG. 7. Franck–Condon simulation of the Si_2H^- spectrum. Parameters given in Table IV.

Fig. 7. The simulation parameters are shown in Table IV. The excellent agreement between these parameters and the calculated values in Table I confirms our assignment. Our term energy of $T_0(^2B_1)=0.020\pm0.005$ eV is in good agreement with the values of 0.02 obtained by Kalcher and Sax[8] and 0.01 eV from our calculations.

C. Si_3H^-

The photoelectron spectrum of Si_3H^- in Fig. 2 shows a single band with a progression of five evenly spaced peaks. The peak spacing is 398 ± 20 cm^{-1}, and the apparent band origin occurs at eKE=0.97 eV. Measurement of the photoelectron angular distributions shows that all five peaks have the same anisotropy parameter of approximately -0.4, indicating they are associated with a single electronic transition.

Theoretical studies on Si_3H and its anion are extremely limited. Kalcher and Sax have performed *ab initio* calculations on Si_3H/Si_3H^- at the CCSD-(T) level of theory.[7] Several structures have been studied for both neutral and anion species. The ground state of the anion is predicted to have a planar cyclic hydrogen-bridged C_{2v} structure as shown in Fig. 5. The valence orbital configuration is $\ldots(11a_1)^2(3b_1)^2(7b_2)^2$, yielding a $^1A_1$ electronic state. The $^2B_2$ ground state of neutral Si_3H, which also has C_{2v} symmetry, is accessed by removal of an electron from the $7b_2$ orbital in the anion. The $7b_2$ orbital and the three totally symmetric vibrational modes of Si_3H/Si_3H^- are shown in Fig. 5. Comparison of Tables I and II shows that the addition of one silicon atom to Si_2H does not lengthen the Si–H bond, but simply enlarges the Si–H–Si angle.

The extended progression in the experimental spectrum indicates a large geometry change between the anion and neutral electronic states. The $^2B_2$ ground state is formed by photodetaching an electron from the $7b_2$ orbital of the anion. Our QCISD(T)/6-31G* calculations show that detachment to the $^2B_2$ state results in a large normal coordinate displacement of $\Delta Q_3=0.42$ Å$\cdot$cm$^{1/2}$. The observed peak spacing of 398 ± 20 cm^{-1} is in good agreement with the ν_3 frequency of 409 cm^{-1} from our calculation (Table II). We therefore assign this band to the $^2B_2$ state. Kalcher and Sax[7] predict the lowest lying excited state with C_{2v} symmetry to lie about 1 eV above the $^2B_2$ ground state; this would not show up in our photoelectron spectrum due to insufficient photon energy. Although other low-lying states are predicted, they have very different geometries from the anion. Photodetachment to these states would result in very extended and broad bands in the photoelectron spectrum. The spectrum thus represents a single electronic transition to the $^2B_2$ ground state, consistent with the photoelectron angular distribution.

TABLE IV. Electron affinities, electronic term values, vibrational frequencies, and normal coordinate changes obtained from Franck–Condon simulation.

	States	T_0 (eV)	Frequencies (cm^{-1})/ΔQ(Å$\cdot$amu$^{1/2}$)									
			ν_1	ΔQ_1	ν_2	ΔQ_2	ν_3	ΔQ_3	ν_5	ΔQ_5	ν_6	ΔQ_6
Si_2H	$^2A_1(C_{2v})$	0.0	1592	0.01	540 $x_2=3^a$	0.12						
EA=2.31±0.01 eV	$^2B_1(C_{2v})$	0.02	1491	0.01	520 $x_2=5^a$	0.23						
Si_3H	$^2B_2(C_{2v})$	0.0	1500	0.02	500	0.02	398 $x_3=2^a$	0.43				
EA=2.53±0.01 eV												
Si_4H^b	$^2A'(C_s)$	0.0	2100	0.05			510	0.64	314	0.79	142	0.18
EA=2.68±0.01 eV												

[a]x_2 and x_3 are the anharmonicities used in the simulations.
[b]The four modes with the largest normal coordinate displacements are used in the simulation.

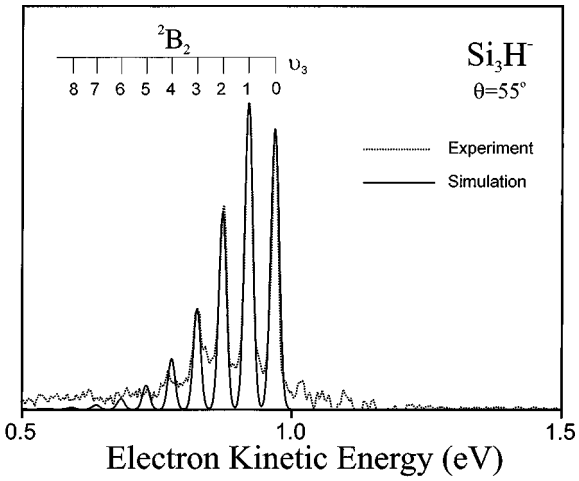

FIG. 8. Franck–Condon simulation of the Si_3H^- spectrum. Parameters given in Table IV.

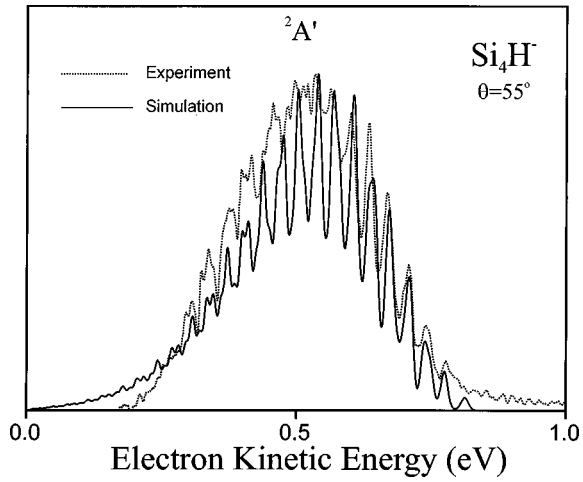

FIG. 9. Franck–Condon simulation of the Si_4H^- spectrum. Parameters given in Table IV.

The Franck–Condon simulation of the $^2B_2$ ground state, using our calculations as a starting point, is shown in Fig. 8. The simulation parameters are shown in Table IV. The normal coordinate displacement, ΔQ_3, used in the simulation is very close to the *ab initio* value in Table II. The vibrational origin at eKE=0.96 eV yields EA(Si_3H)=2.53±0.01 eV for the electron affinity, which lies between the values of 2.65 from Kalcher and Sax and 2.48 eV from our calculations. The electron affinity of Si_3H is 0.24 eV greater than that of Si_3, 2.29 eV.[24]

D. Si_4H^-

No *ab initio* calculations have been published for Si_4H or Si_4H^-. We therefore carried out such calculations on both species in order to better understand the photoelectron spectrum. An initial search for the global minimum energy structures of the anion and neutral was performed at the MP2/6-31G* level of theory. After the ground states of the anion and neutral were located, more accurate electronic state energies were calculated at the QCISD(T) level of theory using the larger 6-311+G(3*DF*) basis set using these geometries. The results are summarized in Table III.

Both the anion and neutral have minimum energy structures of C_s symmetry shown in Fig. 6. The four Si atoms lie in a planar rhombus structure, with the H atom singly bonded to a Si atom (Si_1 in Fig. 6). The optimized geometry shows that the Si_4 unit is distorted, in that the Si–Si bonds involving Si_1 are slightly longer than the other two Si–Si bonds. The hydrogen-bridged structures found in Si_2H and Si_3H are saddle points for Si_4H. The Si–H bond length is 1.535 in Si_4H^- and 1.500 Å in Si_4H, in both cases about 0.15 Å shorter than in the bridged structures for the smaller clusters. For comparison, Si–D single bond lengths are reported to be 1.43 on a Si(111) surface[11] and 1.6±0.2 Å on a Si(100) surface.[10]

The anion $^1A'$ ground state has a valence electron configuration of $\ldots(9a'')^2(18a')^2(19a')^2(20a')^2$. Photodetachment of an electron from the $20a'$ orbital yields the $^2A'$ ground state of the neutral species. The $^2A'$ state has six totally symmetric modes, all of which can be active upon photodetachment. The optimized geometries, vibrational frequencies, and resulting normal coordinate displacements at the QCISD/6-31G* level are shown in Table III. The largest displacement is predicted for the ν_5 mode, which corresponds to a symmetric distortion of the Si_4 framework; this can be seen from the calculated geometries which show the neutral to be more ''square'' than the anion.

The Si_4H^- photoelectron spectrum at 355 nm (Fig. 2) shows a resolved vibrational progression with a peak spacing of 310±20 cm^{-1}. Comparison to Table III shows that this frequency is close to the calculated ν_5 frequency, 334 cm^{-1}. Since this mode has the largest calculated displacement, we assign the observed progression to the ν_5 mode. As shown in Table III, other totally symmetric modes are also active, resulting in a partially resolved progression in the simulated spectrum (Fig. 9). The simulation parameters are shown in Table IV. Only the four modes with the largest displacements were used to perform the Franck–Condon simulation. Moderate adjustments of the ΔQ values from the calculations were made to achieve the best fit to the experimental vibrational profile. Note that ΔQ_1 used in the simulation is substantially less than the calculated value, suggesting a smaller H–Si–Si bond angle change than predicted by the calculation. Also, the experimental and simulated spectra deviate at electron kinetic energies below 0.5 eV, where the contribution of one of the bands from Si_4^- photodetachment is very strong (see Fig. 2). We attribute this deviation to imperfect subtraction of the Si_4^- contribution to the Si_4H^- spectrum.

To obtain the best fit, we chose the vibrational origin at eKE=0.81 eV, yielding EA(Si_4H)=2.68±0.01 eV. Although satisfactory simulations could be generated assuming the vibrational origin to be shifted by a vibrational quantum in either direction, this required using normal coordinate displacements that deviated more from the *ab initio* values. The adiabatic electron affinity from our assignment is 0.15 eV higher than the value of 2.53 eV predicted by our calculation. The electron affinity of Si_4H is 0.55 eV greater than that of Si_4, 2.13 eV.[21]

E. Comparison between Si_n and Si_nH

There are several points of comparison between the photoelectron spectra of Si_nH^- and Si_n^- $(n=2-4)$.[21,23,25,26] The electron affinities of the monohydrides are all slightly larger than those of the corresponding bare clusters. This difference increases with n: 0.11 $(n=2)$, 0.24 $(n=3)$, and 0.55 eV$(n=4)$. There are also similarities between the vibrational structure in the two sets of spectra. Vibrational frequencies of the most active modes are very close for all n. The single band in the Si_3H^- spectrum has a progression of five peaks spaced by 398 cm^{-1}. A progression of similar extent with a peak spacing of 360 cm^{-1} is seen in the Si_3^- spectrum for the transition to the $^3A_2'$ state of Si_3.[25] The Si_4H^- spectrum looks remarkably like the band in the Si_4^- spectrum corresponding to the transition to the $^3B_{3u}$ first excited state, as seen in Fig. 2; the peak spacing is 310 cm^{-1} in both cases. However, there are generally more electronic bands in the Si_n^- spectra over the same energy range.

The similarities in the vibrational progressions suggest that addition of an H atom does not strongly perturb the geometry of the Si_n core, and that the orbitals from which detachment occurs are similar in the bare clusters and monohydrides. This is borne out by the *ab initio* calculations. The Si_3/Si_3^- and Si_4/Si_4^- geometries and vibrational frequencies from previous work[27] are listed at the bottom of Tables II and III for comparison with the monohydrides. In Si_3^-, Si_3H^-, and Si_3H, the Si_3 core is a C_{2v} structure with similar Si–Si bond lengths. The Si_4 core in Si_4H^- and Si_4H is a slightly distorted planar rhombus; Si_4 and Si_4^- have more symmetric D_{2h} planar rhombus structures. The calculations also indicate that the highest occupied molecular orbitals in the monohydride anions are localized on the Si_n core (see Figs. 4–6).

There are, however, differences in the electronic structure of the monohydrides and bare clusters, the most important of which is that the Si_nH^- anions are closed-shell singlets, whereas the Si_n^- clusters are open-shell doublets. This probably accounts for the higher electron affinities of the monohydrides. Si_2^- has two nearly degenerate electronic states separated by only 216.5 cm^{-1},[28] the $X\ ^2\Sigma_g^-$ and $A\ ^2\Pi_u$ states. The Si_2^- photoelectron spectrum[23] shows contributions from both states, but the Si_2H^- spectrum appears to arise from only a single anion electronic state, consistent with the closed-shell configuration of the anion. The molecular orbital configurations of Si_3^- and Si_4^- are $\ldots(3b_1)^2(7b_2)^2(11a_1)^1$ and $(a_g)^2(b_{1u})^2(b_{2g})^1$, respectively. A comparison with the configuration for Si_3H^- (see Sec. IV) indicates that the half-filled 11a orbital in Si_3^- is stabilized by the addition of an H atom and is no longer the highest occupied molecular orbital (HOMO) in Si_3H^-. Instead, the HOMO in Si_3H^- is the $7b_2$ orbital; removal of this electron yields a photoelectron spectrum that resembles the band in the Si_3^- spectrum resulting from detachment from the corresponding orbital, the transition to the $^3A_2'$ state of Si_3. The situation for Si_4H^- is more complicated because of its lower symmetry compared to Si_4^-. The HOMO in Si_4H is the $20a'$ orbital (see Fig. 6), which shares characteristics of the b_{2g} and b_{1u} orbitals in Si_4^-. Nonetheless, the extended progression in the Si_4H^- spectrum is more similar to the band in the Si_4^- spectrum corresponding to the $^3B_{1u}$ excited state of Si_4 than to the ^1A_g ground state.

These considerations also explain the smaller number of electronic bands in the Si_nH^- spectra. In the Si_n^- spectra, photodetachment from the half-filled orbital yields a closed-shell singlet ground state, and photodetachment from the high-lying fully occupied orbitals yields pairs of triplet and singlet excited states. In the Si_nH^- spectra, the transition to the closed-shell singlet is absent, and photodetachment from the HOMO yields one doublet state rather than a triplet–singlet pair.

Finally, we point out that hydrogen atoms form single Si–H bonds on bulk silicon surfaces. The work here shows that bridged structures are more favored for small silicon hydrides such as Si_2H and Si_3H, but that Si_4H has a single Si–H bond. This suggests that Si_4H represents the transition between bridged and single silicon–hydrogen bonds. However, further work on larger clusters is needed to confirm this conjecture.

V. CONCLUSIONS

The anion photoelectron spectra of Si_nH^- $(n=2-4)$ reported here represent the first experimental characterization of the silicon monohydrides. We obtain electron affinities and vibrational frequencies for the Si_nH ground states and for a low-lying excited state of Si_2H. *Ab initio* calculations carried out on the anion and neutral species aid in the assignment of electronic and vibrational spectral features. Our calculations show that the ground states of Si_2H/Si_2H^- and Si_3H/Si_3H^- have planar hydrogen-bridged structures, in agreement with previous theoretical work, but that Si_4H and Si_4H^- have nonbridged C_s structures in which the H atom is bonded to a single silicon atom. The overall good agreement between our experimental spectra and simulations based on the *ab initio* calculations supports the validity of these structures.

The photoelectron spectra of Si_3H^- and Si_4H^- are comprised of vibrationally resolved transitions from the anion to the ground state of the neutral, but in the Si_2H^- spectrum there are strongly overlapped transitions to the ground and first excited state of Si_2H. The two electronic transitions can be distinguished by their photoelectron angular distributions. Comparison with the calculated normal coordinate displacements for the two transitions identifies the ground state as the $^2A_1$ state and the excited state as the $^2B_1$ state with a term value of 0.02 eV.

There are many points of similarity between the Si_nH^- and Si_n^- photoelectron spectra, indicating that the HOMO in the silicon monohydride anions is primarily localized on the Si core; this inference is supported by the *ab initio* calculations. However, the electron affinities of the monohydrides are systematically larger than those of the bare clusters, and the photoelectron spectra of the monohydrides are in general less complex with fewer electronic bands. These trends can be understood by simple molecular orbital considerations.

ACKNOWLEDGMENTS

This work is supported by the National Science Foundation under Grant No. DMR-9521805. Electronic structure calculations were performed at the National Energy Research Scientific Computing Center (NERSC).

[1] J. M. Jasinski, B. S. Meyerson, and B. A. Scott, Annu. Rev. Phys. Chem. **38**, 109 (1987).
[2] G. S. Selwyn, J. Singh, and R. S. Bennett, J. Vac. Sci. Technol. A **7**, 2758 (1989).
[3] A. A. Howling, L. Sansonnes, J.-L. Dorier, and C. Hollenstein, J. Appl. Phys. **75**, 1340 (1994).
[4] M. Bogey, H. Bolvin, C. Demuynck, and J. L. Destombes, Phys. Rev. Lett. **66**, 413 (1991).
[5] B. T. Colegrove and H. F. Schaefer, J. Phys. Chem. **94**, 5593 (1990).
[6] M. M. Huhn, R. D. Amos, R. Kobayashi, and N. C. Handy, J. Chem. Phys. **98**, 7107 (1993).
[7] J. Kalcher and A. F. Sax, Chem. Phys. Lett. **259**, 165 (1996).
[8] J. Kalcher and A. F. Sax, Chem. Phys. Lett. **215**, 601 (1993).
[9] B. Y. Ma, N. L. Allinger, and H. F. Schaefer, J. Chem. Phys. **105**, 5731 (1996).
[10] W. R. Wampler, Phys. Rev. B **51**, 4998 (1995).
[11] W. R. Wampler, Phys. Rev. B **55**, 9693 (1997).
[12] X. Blase, X. J. Zhu, and S. G. Louie, Phys. Rev. B **49**, 4973 (1994).
[13] K. Hricovini, R. Gunther, P. Thiry, A. Talebibrahimi, G. Indlekofer, J. E. Bonnet, P. Dumas, Y. Petroff, X. Blase, X. J. Zhu, S. G. Louie, Y. J. Chabal, and P. A. Thiry, Phys. Rev. Lett. **70**, 1992 (1993).
[14] X. M. Zheng and P. V. Smith, Surf. Sci. **279**, 127 (1992).
[15] Z. Jing and J. L. Whitten, Phys. Rev. B **46**, 9544 (1992).
[16] R. B. Metz, A. Weaver, S. E. Bradforth, T. N. Kitsopoulos, and D. M. Neumark, J. Phys. Chem. **94**, 1377 (1990).
[17] C. Xu, G. R. Burton, T. R. Taylor, and D. M. Neumark, J. Chem. Phys. **107**, 3428 (1997).
[18] D. L. Osborn, D. J. Leahy, D. R. Cyr, and D. M. Neumark, J. Chem. Phys. **104**, 5026 (1996).
[19] J. Cooper and R. N. Zare, in *Lectures in Theoretical Physics*, edited by S. Geltman, K. T. Mahanthappa, and W. E. Brittin (Gordon and Breach, New York, 1969), Vol. XI-C, pp. 317–337.
[20] GAUSSIAN 94, M. J. Frisch, G. W. Trucks, H. B. Schlegel, P. M. W. Gill, B. G. Johnson, M. A. Robb, J. R. Cheeseman, T. Keith, G. A. Petersson, J. A. Montgomery, K. Raghavachari, M. A. Al-Laham, V. G. Zakrzewski, J. V. Ortiz, J. B. Foresman, J. Cioslowski, B. B. Stefanov, A. Nanayakkara, M. Challacombe, C. Y. Peng, P. Y. Ayala, W. Chen, M. W. Wong, J. L. Andres, E. S. Replogle, R. Gomperts, R. L. Martin, D. J. Fox, J. S. Binkley, D. J. Defrees, J. Baker, J. P. Stewart, M. Head-Gordon, C. Gonzalez, and J. A. Pople (Gaussian, Inc., Pittsburgh, PA, 1995).
[21] C. Xu, T. R. Taylor, G. R. Burton, and D. M. Neumark, J. Chem. Phys. **108**, 1395 (1998).
[22] A. F. Sax and J. Kalcher, J. Mol. Struct.: THEOCHEM **67**, 123 (1990).
[23] C. C. Arnold, T. N. Kitsopoulos, and D. M. Neumark, J. Chem. Phys. **99**, 766 (1993).
[24] C. C. Arnold and D. M. Neumark, J. Chem. Phys. **100**, 1797 (1994).
[25] T. N. Kitsopoulos, C. J. Chick, A. Weaver, and D. M. Neumark, J. Chem. Phys. **93**, 6108 (1990).
[26] T. N. Kitsopoulos, C. J. Chick, Y. Zhao, and D. M. Neumark, J. Chem. Phys. **95**, 1441 (1991).
[27] C. M. Rohlfing and K. Raghavachari, J. Chem. Phys. **96**, 2114 (1992).
[28] Z. Liu and P. B. Davies, J. Chem. Phys. **105**, 3443 (1996).